



# Charge asymmetric electrolytes around a rigid cylindrical polyelectrolyte: A generalization of the capacitive compactness



Guillermo Iván Guerrero-García<sup>a,\*</sup>, Lutful Bari Bhuiyan<sup>b</sup>, Christopher W. Outhwaite<sup>c</sup>, Enrique González-Tovar<sup>d</sup>

<sup>a</sup> Facultad de Ciencias de la Universidad Autónoma de San Luis Potosí, Av. Chapultepec 1570, Privadas del Pedregal, 78295 San Luis Potosí, San Luis Potosí, Mexico

<sup>b</sup> Laboratory of Theoretical Physics, Department of Physics, Box 70377, University of Puerto Rico, San Juan, Puerto Rico 00936-8377, USA

<sup>c</sup> Department of Applied Mathematics, University of Sheffield, Sheffield S3 7RH, UK

<sup>d</sup> Instituto de Física de la Universidad Autónoma de San Luis Potosí, Álvaro Obregón 64, Colonia Centro, 78000 San Luis Potosí, San Luis Potosí, Mexico

## ARTICLE INFO

### Article history:

Received 17 May 2022

Revised 4 August 2022

Accepted 2 October 2022

Available online 8 October 2022

### Keywords:

Capacitive compactness

Electrical double layer

Multivalent coions

Ionic specific adsorption

## ABSTRACT

The surface mean electrostatic potential and capacitive compactness of the electrical double layer surrounding an infinite rigid cylindrical polyelectrolyte are analysed for equally-sized  $-1 : z_+$  aqueous electrolytes. Monte Carlo simulations, the non-linear Poisson–Boltzmann equation, the modified Poisson–Boltzmann theory, and the hypernetted chain/mean spherical approximation integral equation are used to examine the role of multivalent cations (coions) when the properties of monovalent anions (counterions) are fixed. A non-zero mean electrostatic potential in the neighbourhood of an uncharged polyelectrolyte is predicted by the simulations and the modified Poisson–Boltzmann theory in the presence of multivalent cations. The concept of capacitive compactness is generalised to overcome the divergence found in the classical definition, when a non-zero potential at the point of zero charge is present. With a highly electrified colloidal surface an inversion is observed, as a function of colloidal charge, in the precedence of the mean electrostatic potential near the polyelectrolyte's surface and of the capacitive compactness between  $-1 : +1$  and  $-1 : z_+$  electrolytes.

© 2022 Elsevier B.V. All rights reserved.

## 1. Introduction

We are honoured to dedicate this paper to Dr. Douglas J. Henderson. Doug was a professional colleague, a teacher, and a friend. His enthusiasm for science was exemplary, his life-long dedication to it inspiring. He will always be a shining star in our collective memory.

The capacitive compactness was proposed by González-Tovar in 2004 [1] to explain an anomalous curvature inversion of the mean electrostatic potential at the Helmholtz plane,  $\Psi_H$ , around a spherical macroion. The anomaly was observed when  $\Psi_H$  was plotted as a function of the colloidal surface charge density, with the macroion being bathed by a  $1 : 1$  or a  $2 : 2$  size-symmetric aqueous electrolyte. Since then, the capacitive compactness has proven to be a versatile concept that allows us to characterize the electrical double layer thickness in charged soft condensed matter systems [2–7]. The main idea behind the capacitive compactness is to define

an effective electrical double layer capacitor associated with a single charged colloidal particle neutralized by a Coulombic fluid. In such a scenario, the separation distance between the real electrode (associated with the charged colloidal particle) and the effective electrical double layer electrode (associated with the centroid of the diffuse ionic charge) is the so-called capacitive compactness (measured from the colloidal surface) [2,4]. In the limit of zero colloidal charge, the capacitive compactness reduces to the Debye length in the framework of the non-linear Poisson–Boltzmann (NLPB) theory of point-ions, in planar and spherical geometries [4]. The well-known dependence of the Debye length on the ionic strength of the supporting Coulombic fluid has been widely used by experimentalists to characterize the thickness of the electrical double layer surrounding a charged colloidal particle in solution [8–10]. One major limitation of this wonted prescription to characterize the spatial extension of the electrical double layer is that the Debye length does not take into account several features typical of charged fluids, viz., the colloidal charge, ion correlations, ionic excluded volume, image charge or polarization effects, and/or ionic specific adsorption. The capacitive compactness, in contrast, encompasses these features, and it is thus a natural generalization of the Debye length. The capacitive compactness has been used to

\* Corresponding author.

E-mail addresses: [givan@uaslp.mx](mailto:givan@uaslp.mx) (G.I. Guerrero-García), [beena@beena.uprrp.edu](mailto:beena@beena.uprrp.edu) (L.B. Bhuiyan), [c.w.outhwaite@sheffield.ac.uk](mailto:c.w.outhwaite@sheffield.ac.uk) (C.W. Outhwaite), [henry@ifisica.uaslp.mx](mailto:henry@ifisica.uaslp.mx) (E. González-Tovar).

characterize the shrinking and expansion of the electrical double layer in valence-asymmetric molten salts and aqueous electrolytes as a function of the colloidal charge, in planar and spherical geometries [4,7]. Alternative definitions of the capacitive compactness in planar, spherical and cylindrical geometries have been recently proposed [6]. These involve the expected value of the electrostatic potential produced by a single electrode in a dielectric medium in the three dimensional space, averaged by a weighting function that depends on the local net charge density of a charged fluid neutralizing an identical electrode under similar conditions of dielectric permittivity.

In planar and spherical geometries, the capacitive compactness depends on the ratio of the mean electrostatic potential at the colloidal surface  $\Psi_0$  divided by the colloidal surface charge density  $\sigma_0$  [4]. In the limit of zero colloidal charge,  $\Psi_0 \rightarrow 0$  in the presence of equisized charge-symmetric  $z : z$  electrolytes due to the expected symmetry of the ionic profiles. This limit is reproduced by the classical NLPB theory. In such a situation, the ratio  $\Psi_0/\sigma_0$  converges to a finite value despite both  $\Psi_0$  and  $\sigma_0$  tend to zero at the point of zero charge. When the ionic symmetry is broken, at the level of the ionic charge and/or at the level of the ionic size, it is possible to observe a non-zero  $\Psi_0$  at the point of zero charge [11–13], often called the potential of zero charge (pzc) in the literature. This pzc is analogous to that observed in experimental systems in the presence of ionic specific adsorption [8,9]. At these asymmetric conditions, the original definition of the capacitive compactness requires revision. In this work, we propose a generalization of the capacitive compactness, which converges in this situation.

On the other hand, in this work we will also study the non-dominance of counterions at the level of the  $\Psi_0$  and of the capacitive compactness  $\tau_c$ , when ion correlations and ionic excluded volume effects are taken into account consistently. According to Valleau and Torrie [14], for the NLPB theory in the limit of very strong electric fields, the ionic size-asymmetry between coions and counterions becomes irrelevant and the only important ion-size parameter is the effective radius of the counterions. In a very recent work [7], it has been explicitly shown, via analytical and numerical calculations, that the electrochemical properties associated with the surface of a planar electrode next to a  $1 : z$  electrolyte, such as the  $\Psi_0$  or the  $\tau_c(\Psi_0, \sigma_0)$ , exactly fulfill the Valleau and Torrie's prescription of the dominance of counterions seen in the NLPB theory. However, in the same article it has also been shown that, in general, the counterions do not necessarily dominate in the planar electrical double layer at the level of electrostatic properties such as the local mean electrostatic potential  $\Psi(x)$  and the electric field  $E(x)$  over the entire extension of the double layer. Specifically, in the limit of an infinite surface charge density it has been demonstrated, via analytical and accurate numerical calculations, that, according to the NLPB picture, the  $\Psi(x)$  and  $E(x)$  do not converge uniformly in the whole space to the same value in the presence of  $1 : z$  electrolytes, even if the properties of monovalent counterions are the same. These results are consistent with primitive model Monte Carlo (MC) simulation data at large bare surface charge densities [4,7]. The qualitative agreement displayed by the NLPB theory regarding the primitive model MC simulations is probably due to the fact that the bulk  $1 : z$  electrolyte with monovalent counterions is still in the weak electrostatic coupling regime, despite the increase of the corresponding ionic strength as a function of the valence  $z$  of the multivalent coions, when the properties of counterions are fixed.

When ion correlations and excluded volume effects are included, it has been proved that the counterions do not entirely dominate or determine the properties of the primitive model electrical double layer over the full diffuse layer [11,12]. In these papers it was found that, at large colloidal charges, the behaviour of the primitive model electrical double layer associated with a

$z : z$  size-asymmetric electrolyte does not correspond to that of a  $z : z$  size-symmetric electrolyte even when the physical attributes of counterions (such as the ionic size, valence, and concentration) are the same in both electrolytes. In other words, the characteristics of the coions in  $z : z$  electrolytes, symmetric in valence but asymmetric in size, are relevant and do matter for highly electrified colloids at high salt concentrations. Furthermore, it has been also proved that in the case of equisized  $1 : z$  primitive model electrolytes with multivalent coions [15], the ionic structure and electrostatic properties of the electrical double layer do not converge, in the limit of very large colloidal surface charge densities, as it would be according to the Valleau and Torrie's dominance of counterions in the classical NLPB approach, in which ion correlations and ionic excluded effects are neglected.

In the present investigation, we will revisit the non-dominance of counterions in cylindrical geometry at the level of the  $\Psi_0$  and of the  $\tau_c$ , when ion correlations and ionic excluded volume effects are considered. These effects are taken into account consistently via MC simulations and theoretical calculations using the MPB theory [16–20] and integral equations under the HNC/MSA closure [11–13,15,21].

## 2. Model, theories and simulations

### 2.1. Model system

In this study, we consider an infinite hard cylinder with radius  $R = 8\text{Å}$  [22] bathed by a binary size-symmetric electrolyte of diameter  $d_+ = d_- = d = 4.25\text{Å}$  and valence  $-1 : z_+$ . An homogeneous surface charge density  $\sigma_0 \geq 0$  is considered in all cases. As a result, counterions are always monovalent and coions can be monovalent or multivalent. The whole system is immersed in a continuum solvent with dielectric constant  $\epsilon = 78.5$  and temperature  $T = 298\text{K}$ . In the presence of ion correlations, that is, for MC simulations, the MPB equation and HNC/MSA integral equation, all ionic species are treated as hard spheres with point charges in their centers, which constitute the so-called primitive model (PM). In such an approach, the interaction potential between an ion  $i$  and an ion  $j$  can be written as

$$u_{ij}(r_{ij}) = \begin{cases} \infty, & \text{if } r_{ij} < d, \\ \frac{z_i z_j e^2}{4\pi\epsilon_0 \epsilon r_{ij}}, & \text{if } r_{ij} \geq d, \end{cases} \quad (1)$$

where  $r_{ij} = |\mathbf{r}_i - \mathbf{r}_j|$ ,  $e$  is the proton charge,  $\epsilon_0$  is the vacuum permittivity, and  $\epsilon$  is the dielectric constant of the solvent. When the diameter of all the ionic species is the same (i.e.,  $d_+ = d_- = d$ ), this representation of the electrolyte is known as the *restricted primitive model* (RPM). For the NLPB the Stern correction is incorporated.

The interaction between an ion  $i$  and the charged cylinder in the RPM, and also for the NLPB equation with Stern correction, is given by:

$$u_i(r'_i) = \begin{cases} \infty, & \text{if } r'_i < R + \frac{d}{2}, \\ -\frac{z_i e \lambda}{2\pi\epsilon_0 \epsilon} \ln(r'_i) + C, & \text{if } r'_i \geq R + \frac{d}{2}, \end{cases} \quad (2)$$

where  $C$  is an arbitrary constant that can be used to define the zero of the electrostatic potential and to reduce the argument of the logarithm,  $\lambda$  is the linear charge density per unit length of the infinite rigid charged cylinder, with an associated surface charge density  $\sigma_0$ , and  $r'_i$  is the perpendicular distance of an ion  $i$  to the line of charge placed at the center of the hard cylinder.

2.2. The Poisson–Boltzmann and the modified Poisson–Boltzmann equations

The Poisson equation for the mean electrostatic potential  $\Psi(r)$  at a perpendicular distance  $r$  from the cylinder axis reads

$$\nabla^2\Psi(r) = -\frac{e}{\epsilon_0\epsilon} \sum_s z_s \rho_s g_s(r), \tag{3}$$

where  $g_s(r) = \rho_s(r)/\rho_s$  is the cylinder-ion singlet distribution function for the ion species  $s$ , with  $\rho_s$  being the bulk density of the same ions species. In the Boltzmann approximation  $g_s(r) = \exp(-ez_s\beta\Psi(r))$ , where  $\beta = 1/(k_B T)$ ,  $k_B$  is the Boltzmann constant and  $T$  the temperature. Substituting this  $g_s$  in the above equation leads to the NLPB equation, which in the present cylindrical symmetry can be written as

$$\frac{1}{r} \frac{d}{dr} \left( r \frac{d\Psi(r)}{dr} \right) = -\frac{e}{\epsilon_0\epsilon} \sum_s z_s \rho_s \exp(-ez_s\beta\Psi(r)). \tag{4}$$

The mean field nature of the classical PB theory is apparent from the fact that the inter-ionic correlations are neglected. The other important drawback is that the ions are treated as point ions so that all ionic exclusion volume effects are ignored. Within the potential approach these deficiencies are taken into account in the MPB theory described below.

The MPB equation appropriate for a cylindrical double layer was derived by Outhwaite [16]. Further work was done by Bhuiyan and Outhwaite [17–19] in the early 1990s and later. We sketch here the principal equations of the theory.

The MPB cylinder-ion singlet profile  $\rho_s(r) = \rho_s g_s(r)$  can be written as

$$\rho_s(r) = \rho_s \zeta_s(r) \exp \left[ -\frac{\beta q_s^2}{2\epsilon_0\epsilon d} (F - F_0) - \frac{\beta q_s F}{2\sqrt{r}} \{u(r+d) + u(r-d)\} + \frac{\beta q_s(F-1)}{2d\sqrt{r}} \int_{r-d}^{r+d} u(R) dR \right], \tag{5}$$

where  $u(r) = \sqrt{r} \Psi(r)$ .

$$F = \begin{cases} 1/\{(1 + \kappa d) - (\kappa d/\pi)S\} & R + d/2 \leq r \leq R + 3d/2, \\ 1/(1 + \kappa d) & r \geq R + 3d/2, \end{cases} \tag{6}$$

$$F_0 = \lim_{r \rightarrow \infty} F = 1/(1 + \kappa_D d), \tag{7}$$

with

$$S = \int_{\theta_0}^{\pi/2} \sin \theta \cos^{-1} \left\{ \frac{c - \cos^2 \theta}{(2r/d) \sin \theta} \right\} d\theta, \tag{8}$$

$$\theta_0 = \sin^{-1} \left[ \frac{r - (R + d/2)}{d} \right], \tag{9}$$

$$c = 1 - \left( \frac{R}{d} + \frac{1}{2} \right)^2 + \left( \frac{r}{d} \right)^2, \tag{10}$$

with  $\kappa$  and  $\kappa_D$  being the local and bulk Debye–Hückel parameters

$$\kappa^2 = \frac{e^2 \beta}{\epsilon_0 \epsilon} \sum_s z_s^2 \rho_s(r), \tag{11}$$

$$\kappa_D = \lim_{r \rightarrow \infty} \kappa. \tag{12}$$

The exclusion volume term  $\zeta_s(r)$  is the same as for the planar double layer [23]. This approximation has proved reasonable in earlier works. [17–19]

$$\zeta_s(r) = \rho_s(r|q_s = 0)/\rho_s = \Theta(r - (R + d/2)) \exp \left[ 2\pi \int_r^\infty \sum_\gamma \int_{\max(R+d/2, y-d)}^{y+d} (x-y) \rho_\gamma(x) \exp \left\{ -\beta q_\gamma \phi(y, x) \right\} dx dy \right], \tag{13}$$

$$\phi(y, x) = \frac{F}{4\pi d} \int_V \nabla^2 \Psi dV \tag{14}$$

$\Theta(x)$  is the Heaviside function, while  $\phi(y, x)$  is the fluctuation potential evaluated on the exclusion surface of the discharged ion. The MPB theory is seen to reduce to the nonlinear PB theory upon taking  $\zeta_s(r) = 1, F = F_0$  and  $d \rightarrow 0$ . The MPB theory was solved numerically using a quasi-linearization iterative procedure [24,25].

As indicated before, this planar double layer formulation of the  $\zeta(x)$  was found to be a good approximation in cylindrical symmetry (Refs. [17–19]) at the model parameters used, which were very similar to those employed here. Dorvilien et al. [19] noted very good agreement between the MPB  $\Psi(r)$  and  $g_s(r)$  with the corresponding MC simulations. We further emphasize the fact that the shape of the ions, however, is independent of the geometry of the double layer, and remains spherical. In all applications of the MPB in planar, cylindrical, and spherical symmetries [39], the formulation of the exclusion volume term treats the ions as charged hard spheres.

2.3. Integral equations theory in the HNC/MSA approximation

The HNC/MSA integral equation is based on the multicomponent Ornstein–Zernike equation for 3 species, with one species  $M$  corresponding to the single, infinite and uniformly charged cylindrical colloid and the remainder being the two RPM ion species. Since the quantity of interest is the distribution of ions around the cylinder, the Ornstein–Zernike equation is expressed in terms of total and the pair correlation functions, which are related by  $h_{Mj}(r) = g_{Mj}(r) - 1$ . To obtain a closed system, from the fundamental Ornstein–Zernike equation, the HNC approximate closure is used for the colloid-ion direct correlation function  $c_{Mj}(r)$  and the bulk MSA closure for the analytic ion-ion direct correlation function  $c_{kj}(r)$  [26], where  $M, j, k$  represent the colloid and ions, respectively. This leads to the following result, dropping the subscript  $M$ ,

$$g_j(r) = \exp \left\{ -\beta u_j(r) + \sum_{k=+,-} \rho_k \int [g_k(t) - 1] c_{kj}^{MSA}(s) d^3 t \right\}. \tag{15}$$

In a previous paper by one of the present authors [21], the integral in the RHS of the previous equation has been performed in cylindrical coordinates and, consequently, the following detailed expression for the pair of HNC/MSA integral equations of the cylindrical electrical double layer, for a constant surface electrostatic potential  $\Psi_0$ , has been given, namely

$$g_j(r) = \exp \left\{ -z_j e \beta \Psi_0 + z_j \int_{R+(d/2)}^\infty f^{[\Psi_0]}(r, t) \bar{\rho}_d(t) dt + z_j \int_{R+(d/2)}^\infty K_d(r, t) \bar{\rho}_d(t) dt + \int_{R+(d/2)}^\infty K_s(r, t) \bar{\rho}_s(t) dt + \rho A(r) \right\}, \tag{16}$$

with  $j = +, -$  and  $r \geq R + (d/2)$ ,

$$f^{|\Psi_0|}(r, t) = \frac{\beta e^2}{2\epsilon_0\epsilon} t \ln \left[ \frac{R^2(r^2 + t^2 + |r^2 - t^2|)}{2r^2t^2} \right], \quad (17)$$

$$\rho = \sum_{k=+,-} \rho_k, \quad (18)$$

$$\bar{\rho}_s(t) = \sum_{k=+,-} \rho_k [g_k(t) - 1], \quad (19)$$

$$\bar{\rho}_d(t) = \sum_{k=+,-} z_k \rho_k [g_k(t) - 1], \quad (20)$$

$$K_s(r, t) = -4t \int_0^{\phi_0} \left[ c_1 J_0(\phi) + 6\eta c_2 J_1(\phi) + \frac{1}{2} \eta c_3 J_3(\phi) \right] d\phi, \quad (21)$$

for  $|r - t| \leq d$  and  $K_s(r, t) = 0$  for  $|r - t| > d$ ,

$$A(r) = - \int_0^{R+(d/2)} K_s(r, t) dt, \quad (22)$$

for  $r \leq R + (3d/2)$ , and

$$K_d(r, t) = \frac{e^2 \beta}{\pi \epsilon_0 \epsilon} t \int_0^{\phi_0} \left[ J_2(\phi) - \frac{2\Gamma J_0(\phi)}{(1 + \Gamma d)} + \frac{\Gamma^2 J_1(\phi)}{(1 + \Gamma d)^2} \right] d\phi, \quad (23)$$

for  $|r - t| \leq d$  and  $K_d(r, t) = 0$  for  $|r - t| > d$ . In the previous equations

$$\eta = \frac{1}{6} \pi \rho d^3, \quad (24)$$

$$c_1 = \frac{(1 + 2\eta)^2}{(1 - \eta)^4}, \quad (25)$$

$$c_2 = - \frac{(1 + (\eta/2))^2}{d(1 - \eta)^4}, \quad (26)$$

$$c_3 = \frac{1}{d^3} c_1, \quad (27)$$

$$\Gamma d = -\frac{1}{2} + \frac{1}{2} \sqrt{1 + 2\kappa_D d}, \quad (28)$$

$$\phi_0 = \arccos \left[ \frac{r^2 + t^2 - d^2}{2rt} \right], \quad (29)$$

$$Z_0(\phi) = (d^2 - r^2 - t^2 + 2rt \cos \phi)^{1/2}, \quad (30)$$

$$S_0(\phi) = (r^2 + t^2 - 2rt \cos \phi)^{1/2}, \quad (31)$$

$$J_0(\phi) = Z_0(\phi), \quad (32)$$

$$J_1(\phi) = \frac{1}{2} d Z_0(\phi) + \frac{1}{2} [S_0(\phi)]^2 J_2(\phi), \quad (33)$$

$$J_2(\phi) = \ln \left( \frac{d + Z_0(\phi)}{S_0(\phi)} \right) \quad (34)$$

and

$$J_3(\phi) = \frac{1}{4} d Z_0(\phi) \left[ d^2 + \frac{3}{2} [S_0(\phi)]^2 \right] + \frac{3}{8} [S_0(\phi)]^4 J_2(\phi). \quad (35)$$

It must be noted that, if the interionic correlations due to the finite size of the ions are neglected in Eq. (16),  $K_s(r, t) = K_d(r, t) = 0$  everywhere and, thus, such equation becomes

$$g_j(r) = \exp \left\{ -z_j e \beta \Psi_0 + z_j \int_{R+(d/2)}^{\infty} f^{|\Psi_0|}(r, t) \bar{\rho}_d(t) dt \right\}, \quad (36)$$

for  $r \geq R + (d/2)$ . The prior expression represents, in fact, the integral equation version of the celebrated Poisson–Boltzmann differential equation (see Eq. (4)), for cylindrical geometry and constant  $\Psi_0$ , supplemented with the so-called Stern layer correction.

Noticeably, in this paper we will investigate systems of cylindrical double layers with a constant surface charge density,  $\sigma_0$ . Thus, it is convenient, for numerical calculation purposes, to recast Eq. (16) in terms of  $\sigma_0$ . The resulting HNC/MSA system of integral equations is

$$g_j(r) = \exp \left\{ -z_j \left( \frac{\beta e R}{\epsilon_0 \epsilon} \right) \ln \left[ \frac{R}{R+(d/2)} \right] \sigma_0 + z_j \int_{R+(d/2)}^{\infty} f^{|\sigma_0|}(r, t) \bar{\rho}_d(t) dt + z_j \int_{R+(d/2)}^{\infty} K_d(r, t) \bar{\rho}_d(t) dt + \int_{R+(d/2)}^{\infty} K_s(r, t) \bar{\rho}_s(t) dt + \rho A(r) \right\}, \quad (37)$$

where  $r \geq R + (d/2)$ ,  $j = +, -$ , and

$$f^{|\sigma_0|}(r, t) = \frac{\beta e^2}{2\epsilon_0\epsilon} t \ln \left[ \frac{(R + (d/2))^2 (r^2 + t^2 + |r^2 - t^2|)}{2r^2 R^2} \right]. \quad (38)$$

Correspondingly, if the interionic correlations due to the finite size of the ions are not taken into account in Eq. (37), this equation turns into

$$g_j(r) = \exp \left\{ -z_j \left( \frac{\beta e R}{\epsilon_0 \epsilon} \right) \ln \left[ \frac{R}{R+(d/2)} \right] \sigma_0 + z_j \int_{R+(d/2)}^{\infty} f^{|\sigma_0|}(r, t) \bar{\rho}_d(t) dt \right\}, \quad (39)$$

which is the integral equation form of the Poisson–Boltzmann differential equation, for cylindrical geometry and constant  $\sigma_0$ , with the Stern layer correction.

To obtain the results reported below, the system of integral equations for the electrical double layer in cylindrical geometry, given by Eq. (37), was solved numerically via a robust and efficient Finite Element method. The details of the application of such a technique can be consulted elsewhere [27,28].

#### 2.4. Monte Carlo simulations

The electric field produced by the infinite rigid charged cylinder of radius  $R$  beyond its surface is equivalent to that generated by an infinite line of charge of density  $\lambda$ , which is placed in the center of the cylinder along its symmetry axis. In order to compare simulation data and theoretical results, we have placed  $N_{cyl}$  equally spaced point-charges  $q_s = e/10$  along the cylinder's symmetry axis of length  $L$  [22], where  $e$  is the proton charge. As a result, the linear charge of density per unit length and the corresponding surface charge density are defined, respectively, as

$$\lambda = \frac{N_{cyl} q_s}{L} \quad (40)$$

and

$$\sigma_0 = \frac{N_{cyl} q_s}{2\pi R L}. \quad (41)$$

The interaction between an ion  $i$  of diameter  $d$  and a point-charge  $q_s$  located along the line of charge located at the symmetry axis of the cylinder is given by

$$u_{ij}^*(r'_i, r'_{is}) = \begin{cases} \infty, & \text{for } r'_i < R + \frac{d}{2}, \\ \frac{e z_i q_s}{4\pi \epsilon_0 \epsilon r'_{is}}, & \text{for } r'_i \geq R + \frac{d}{2}, \end{cases} \quad (42)$$

where  $r'_i$  is the perpendicular distance of an ion  $i$  to the line of charge placed at the center of the hard cylinder,  $r_{is} = |\mathbf{r}_i - \mathbf{r}_s|$  is the distance between an ion  $i$  (of charge  $ez_i$ ) and a point-charge  $q_s$  located along the line of charge.

A cubic simulation box of length  $L$  with periodic boundary conditions has been used to perform  $NVT$  Monte Carlo simulations via the Metropolis algorithm [29,30]. In order to avoid border effects, the length  $L$  is several times the Debye length of the supporting electrolyte. In typical runs, from 4,000 to 7,000 particles have been placed in the simulation box. The total number of ions is also adjusted to obtain the desired bulk concentration far away from the cylinder surface, but always fulfilling the electroneutrality condition, i.e.,

$$\sum_{s=1}^{N_{cyl}} q_s + N_c z_- e + N_+ z_+ e + N_- z_- e = 0 \quad (43)$$

where  $N_{cyl}$  is the number of discrete charges placed on the line of charge,  $N_c$  and  $z_-$  are the number and valence of free counterions of the line of charge, and  $N_k$  and  $z_k$ , for  $k = +, -$ , are the number of ions and the valence corresponding to the ionic species  $k$  constituting the supporting electrolyte, respectively.

The integrated linear charge per unit length can be defined as

$$Q(r) = \lambda + 2\pi \sum_{i=+,-} \int_R^r ez_i \rho_i(t) dt, \quad (44)$$

and the mean electrostatic potential as a function of  $r$  is given by

$$\Psi(r) = \int_r^\infty \frac{1}{2\pi\epsilon_0\epsilon} \frac{Q(t)}{t} dt \quad (45)$$

for  $r \geq R$ . In particular, the mean electrostatic potential at the surface and at the Helmholtz plane are given by  $\Psi_0 = \Psi(r=R)$  and  $\Psi_H = \Psi(r=R+d/2)$ , respectively. The above definitions of the integrated linear charge per unit length and mean electrostatic potential as a function of the perpendicular distance to the cylinder's surface are valid for Monte Carlo simulations and for the theoretical calculations using the NLPB equation, the MPB theory, and integral equations with the HNC/MSA closure.

Several computational schemes alternative to Ewald sums have been proposed to properly handle long-ranged Coulombic interactions [31–36]. In this work, we have used the classical Ewald sums approach [29,30] with a damping constant  $\alpha = 5/L$  (where  $L$  is the length of the cubic simulation box) and 725 vectors in the  $k$ -space to compute the reciprocal space contribution to the total electrostatic energy (details of the implementation are discussed elsewhere [12,13,37]). In all MC simulations, at least  $2 \times 10^5$  MC cycles were executed for thermalization, and from  $1 \times 10^6$  to  $2 \times 10^6$  MC cycles have been performed to calculate the canonical average.

## 2.5. Generalization of the capacitive compactness in the presence of a non-zero surface electrostatic potential at the point of zero charge

From the physical definition of a conventional capacitor, the difference of the electrostatic potential between the electrodes is produced by the surface charge on the electrodes. By the electroneutrality condition, the charge on an effective electrode associated to the diffuse electrical double layer is of the same magnitude and opposite sign regarding the charge present at the electrode associated to the colloidal surface. In the absence of charge at the colloidal surface, a zero charge is expected at the effective electrode associated to the diffuse electrical double layer. However, notice that a mean electrostatic potential different from zero could be observed at the surface of a neutral colloid, due to a spatial distribution of charge associated to the diffuse electrical double layer,

which might result from ionic size and/or charge asymmetry, ion correlations, polarization effects, ionic specific adsorption, etc.

On the other hand, in previous works [2–7], the capacitive compactness in cylindrical, planar, and spherical geometries have been defined, in general, as:

$$\tau_{c,cylinder} = R \exp\left(\frac{\epsilon_0 \epsilon \Psi_0}{R \sigma_0}\right) \quad (46)$$

$$\tau_{c,wall} = \frac{\epsilon_0 \epsilon \Psi_0}{\sigma_0} \quad (47)$$

$$\tau_{c,sphere} = R_{sphere} \left[1 - \left(\frac{\epsilon_0 \epsilon \Psi_0}{R_{sphere} \sigma_0}\right)\right]^{-1}. \quad (48)$$

In these definitions, it has been assumed that the mean electrostatic potential at the colloidal surface tends to zero when the colloidal surface charge density goes also to zero, although the ratio of both quantities has a finite value. These conditions are fulfilled, for instance, by the non-linear Poisson–Boltzmann theory of point ions, with symmetric valences  $z : z$  and equal closest ionic approach distances to the colloidal surface. Thus, Eqs. (46)–(48) can be used to calculate the capacitive compactness for any surface charge density  $\sigma_0$ . In the presence of a spherical or a planar neutral electrode the NLPB theory reduces to the Debye–Hückel formalism, and the capacitive compactness is equal to

$$\tau_{c,wall}^{DH} = \frac{1}{\kappa_D} = \lambda_D \quad (49)$$

$$\tau_{c,sphere}^{DH} = \frac{1}{\kappa_D} = \lambda_D \quad (50)$$

where  $\lambda_D$  is the well-known Debye length,

$$\lambda_D^{-1} = \kappa_D = \left(\frac{\sum_i \rho_i^{bulk} z_i^2 e^2}{\epsilon_0 \epsilon k_B T}\right)^{\frac{1}{2}}, \quad (51)$$

which only depends on the bulk properties of the electrolyte. For the case of a cylindrical electrode with radius  $R$ , the respective capacitive compactness is equal to the Debye length but now multiplied by a factor that depends on dimensionless parameter  $\kappa_D R$ , i.e.,

$$\tau_{c,cylinder}^{DH} = \lambda_D \left[ (\kappa_D R) \times \exp\left(\frac{J_0(\kappa_D R)}{\kappa_D R J_1(\kappa_D R)}\right) \right], \quad (52)$$

with  $J_0$  and  $J_1$  being the zero and first order modified Bessel functions of the second kind, respectively [9]. Notice that in the case of the NLPB theory with symmetric valences  $z : z$  and equal closest ionic approach distances to the colloidal surface (mentioned above), for these three geometries of neutral electrodes, the mean electrostatic potential at the colloidal surface is zero by symmetry. Interestingly, the corresponding ratio of these last two quantities is finite and well defined in the limit of a zero colloidal surface charge. This behaviour is also physically expected in more sophisticated statistical mechanics approaches and/or molecular simulations for systems with fully-symmetric electrolytes.

Contrastingly, if the mean electrostatic potential at the colloidal surface is finite when the colloid is uncharged, the capacitive compactness given by Eqs. (46)–(48) presents a singularity. Thus, we propose here that the mean electrostatic potential at the colloidal surface  $\Psi_0(\sigma_0)$  be replaced by this quantity minus the surface mean electrostatic potential when the colloid is uncharged (this last quantity being the pzc):

$$\widetilde{\Psi}_0(\sigma_0) = \Psi_0(\sigma_0) - \Psi_0(\sigma_0 = 0). \quad (53)$$

Then, the capacitive compactness in cylindrical, planar, and spherical geometries can be still calculated by using Eqs. (46)–(48), after replacing  $\Psi_0(\sigma_0)$  by  $\tilde{\Psi}_0(\sigma_0)$ . From a physical point of view, Eq. (53) is justified by considering that two solutions ( $\Psi(r)$  and  $\tilde{\Psi}(r)$ ) of the Poisson equation of electrostatics

$$\nabla^2 \Psi(r) = \frac{\rho(r)}{\epsilon_0 \epsilon} \quad (54)$$

can differ at most by a constant. By convention, the mean electrostatic potential  $\Psi(r)$  is usually defined as zero very far away from the charged colloidal surface, for an arbitrary surface charge density  $\sigma_0$ . In Eq. (53), the mean electrostatic potential  $\tilde{\Psi}(r)$  is defined as zero when  $r = R$  and  $\sigma_0 = 0$ .

On the other hand, notice that a pzc can be observed experimentally in the presence of specific ionic adsorption [8,9]. In the absence of specific ionic adsorption, a finite pzc has also been observed for systems with size-asymmetric ions [11–13]. In this work, we show that a finite pzc can be observed in the presence of equally sized ions with asymmetric valences. Other interesting consequences of breaking the ionic asymmetry in size and/or valence in the absence of specific ionic adsorption have been discussed in a recent review [38].

From the physical arguments discussed above, it is expected that the Eq. (53) be valid at least in cylindrical, planar, and spherical geometries if the pzc is finite. In the absence of a pzc, the capacitive compactness is well defined if the ratio  $\Psi_0(\sigma_0)/\sigma_0$  is finite, as occurs in the NLPB theory and in integral equations theory in the HNC/MSA approximation in size-symmetric and valence asymmetric electrolytes as it is exhibited below.

### 3. Results and discussion

Given that the mean electrostatic potential at the colloidal surface and that at the Helmholtz plane are related by the equation  $\Psi_0(\sigma_0) = \frac{\lambda}{2\pi\epsilon_0\epsilon} \ln\left(1 + \frac{d/2}{R}\right) + \Psi_H(\sigma_0)$ , we will discuss the behaviour of  $\Psi_H(\sigma_0)$ , instead of  $\Psi_0(\sigma_0)$ , in order to emphasize the curvature variation of the  $\Psi_H$ , as a function of the valence asymmetry. We begin by displaying in Fig. 1 the function  $\Psi_H(\sigma_0)$  for several  $-1 : z_+$  electrolytes. This property has been obtained via MC simulations, the NLPB equation, the MPB theory, and the integral equations theory in the HNC/MSA approximation. In Fig. 1(a) it is seen that, in the presence of a size- and charge-symmetric  $-1 : +1$  electrolyte,  $\Psi_H = 0$  at  $\sigma_0 = 0$  according to both the simulations and theories as can be observed in the corresponding inset. Physically, if the colloid is neutral, this behaviour is expected because in an all-symmetric (in ionic size and valence) binary electrolyte the ionic profiles of cations and anions are identical near the colloidal surface. When  $\sigma_0$  increases,  $\Psi_H$  increases monotonically for MC and the theories. The MPB results correspond very well to the MC simulations data. Contrastingly, at large  $\sigma_0$  values, the NLPB equation results overestimate  $\Psi_H$ , whereas the HNC/MSA integral equations data underestimate  $\Psi_H$ .

Fig. 1(b) illustrates the case for a size-symmetric but charge-asymmetric  $-1 : +2$  electrolyte. The  $\Psi_H$  displays a non-zero value at  $\sigma_0 = 0$  according to MC simulations and the MPB theory, whereas the NLPB and HNC/MSA results predict a zero  $\Psi_H$  at  $\sigma_0 = 0$  (see the corresponding inset). The breaking of the valence symmetry promotes an asymmetric ionic adsorption at the colloidal surface, as shown in the Figs. 2 (a) and 3(a) for  $-1 : +2$  and  $-1 : +3$  electrolytes, respectively. The MPB distribution functions have a discontinuity in the gradient at  $r = R + 3d/2$ . Increasing the surface charge ameliorates this failure, see the radial distribution plots in references [17–19]. The gradient discontinuity arises because it is not possible to satisfy accurately the fluctuation

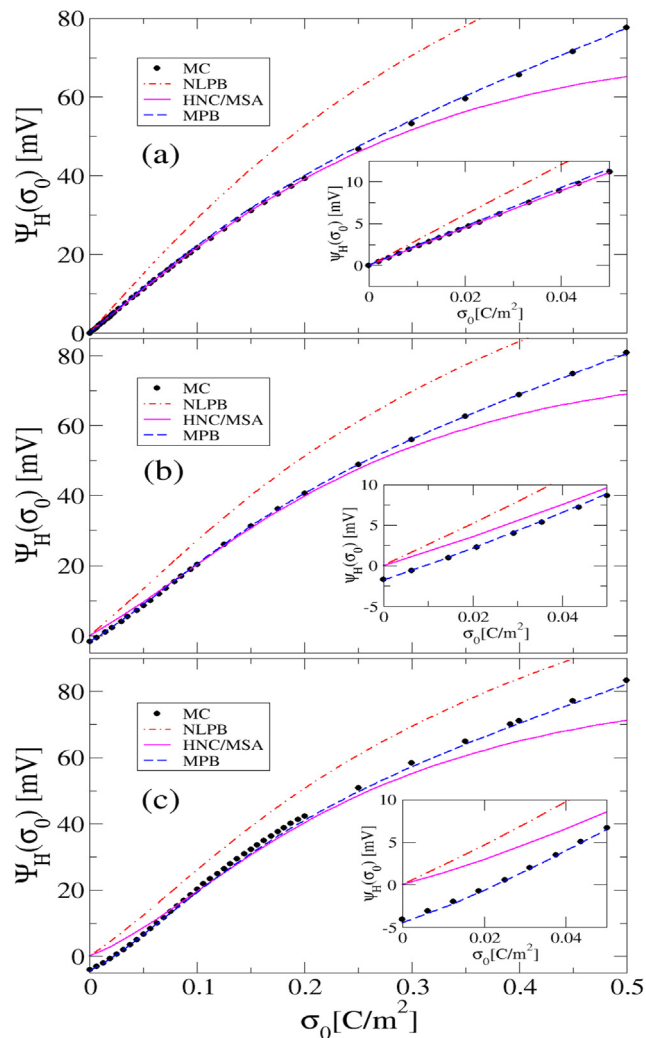


**Fig. 1.** (Color online): Mean electrostatic potential at the Helmholtz plane,  $\Psi_H$ , as a function of the surface charge density,  $\sigma_0$ , in the presence of the following  $-1 : z_+$  electrolytes: (a)  $-1 : +1$ ; (b)  $-1 : +2$ ; and (c)  $-1 : +3$ . Solid circles, dot-dashed lines, solid lines and dashed lines correspond to MC simulations, NLPB equation, integral equations in the HNC/MSA, and the MPB theory, respectively. The monovalent anions have the same concentration  $\rho^{bulk} = 1\text{M}$  in all instances, and the concentration of cations is adjusted, accordingly, in order to fulfill the electroneutrality condition as a function of their valence  $z_+$ .

potential boundary conditions at the intersection of the cylinder/ion exclusion volumes with an approximate fluctuation potential. This discontinuity also occurs for the planar and spherical double layers, but it does not arise for the bulk situation where the fluctuation potential boundary conditions are satisfied.

The asymmetric ionic adsorption means that the corresponding net ionic charge density per unit volume is also different from zero near the surface of an uncharged colloid. This produces a non-zero mean electrostatic potential in the region located between the colloidal surface and the Helmholtz plane, as shown in Figs. 2(b) and 3 (b). The MC and MPB values of  $\Psi_0$  at  $\sigma_0 = 0$  for the  $-1 : +2$  and the  $-1 : +3$  electrolytes are shown in Table 1. In the case of the NLPB and HNC/MSA theories, both theoretical approaches predict a zero mean electrostatic potential over the entire extension of the electrical double layer when  $\sigma_0 = 0$ . On the other hand,  $\Psi_H$  increases monotonically when  $\sigma_0$  increases as it is observed in Fig. 1(b). However, a change of curvature is predicted by simulations and all the theories as a function of  $\sigma_0$  in the presence of a  $-1 : +2$  electrolyte. As before for the  $-1 : +1$  electrolyte displayed in Fig. 1(a),

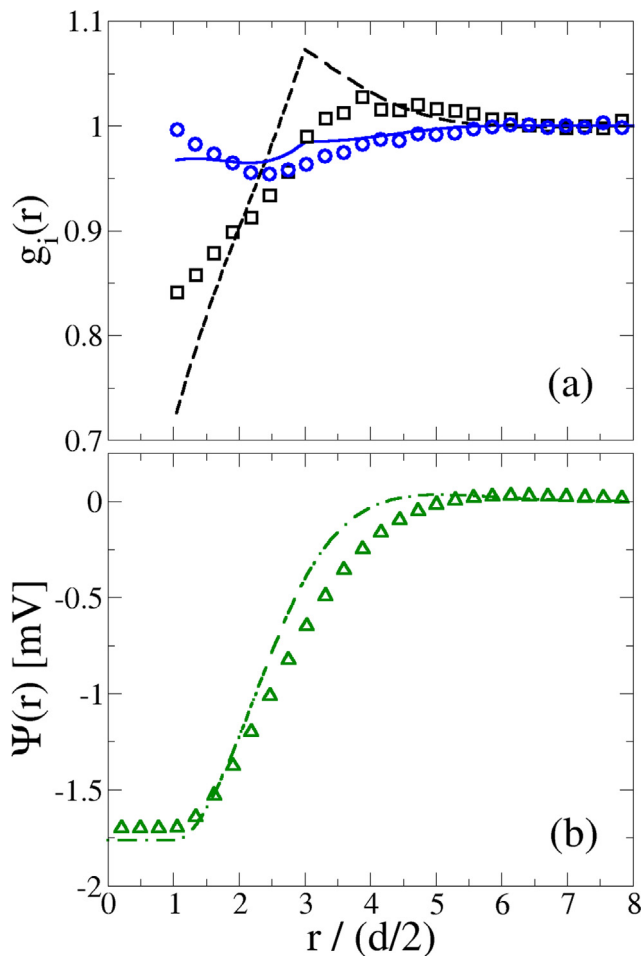


**Fig. 2.** (Color online): (a) Radial distribution function (RDF),  $g_i(r)$ , and (b) mean electrostatic potential,  $\Psi(r)$ , as a function of the distance to the surface of an infinite uncharged cylinder immersed in a  $-1:+2$  electrolyte. Symbols and lines correspond to MC simulations and the MPB theory, respectively. The blue circles and the blue solid line correspond to the RDF of monovalent anions; the black squares and the black dashed line correspond to the RDF of divalent cations; the green triangles and the green dot-dashed line are associated to the mean electrostatic potential. The monovalent anions have a concentration  $\rho^{bulk} = 1M$ , and the concentration of cations is adjusted, accordingly, in order to fulfill the electroneutrality condition as a function of their valence  $z_+$ .

the MPB results agree very well with MC simulations data, whereas the NLPB equation results overestimate  $\Psi_H$ , and the HNC/MSA data underestimate  $\Psi_H$  at large  $\sigma_0$  values.

The  $-1 : +3$  electrolyte results for  $\Psi_H(\sigma_0)$  are given in Fig. 1(c). This plot shows that the deviation from the  $-1 : +1$  system parallels that for the  $1 : 2$  electrolyte, whereas the increase of the coion valency from 2 to 3 augments the magnitude of  $\Psi_H$  at  $\sigma_0 = 0$ . Again, when  $\sigma_0$  increases, the  $\Psi_H$  displays a behaviour similar to that observed in the presence of a  $-1 : +2$  electrolyte in Fig. 1(b):  $\Psi_H$  shows a change of curvature as a function of  $\sigma_0$  and the MPB results agree very well with MC simulations data, whereas the NLPB and HNC/MSA results overestimate and underestimate the  $\Psi_H$  at large  $\sigma_0$  values, respectively.

In Fig. 4, the capacitive compactness  $\tau_c$  plots corresponding to the  $\Psi_H$  curves of Fig. 1 are displayed. In particular, notice that the capacitive compactness  $\tau_c$  is well defined for the  $-1 : +1$  electrolyte in the limit of  $\sigma_0 \rightarrow 0$ , being  $\Psi_0(\sigma_0 = 0) = 0$  due to the symmetry in the size and valence of the binary electrolyte (see Fig. 4(a)). In the present instance,  $\tau_c$  decreases monotonically as a function of  $\sigma_0$  according to MC simulations, the NLPB equation, the MPB theory, and the HNC/MSA integral equations. As it has been shown in a previous work in planar and spherical geometry [4],

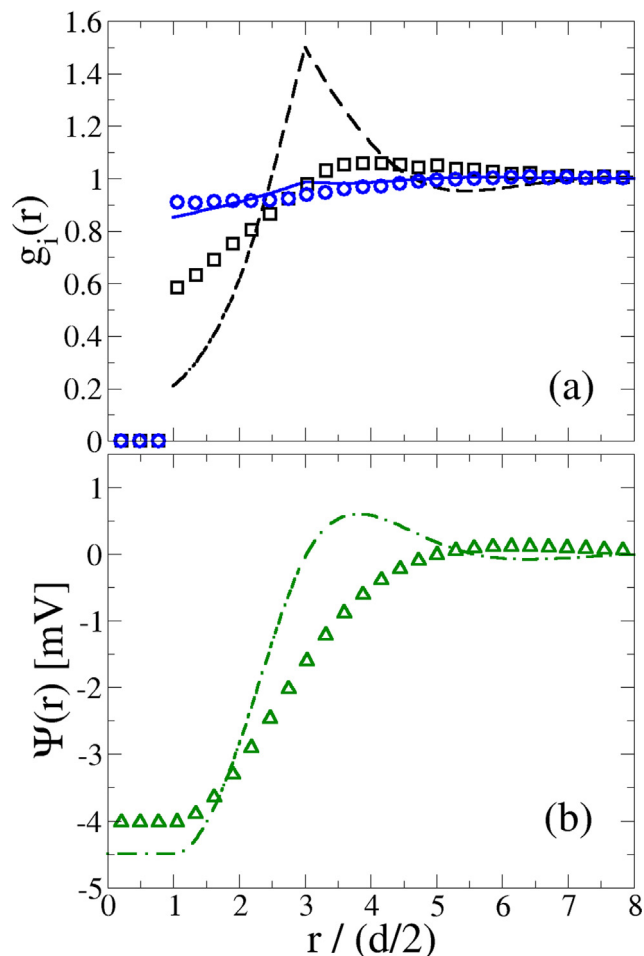


**Fig. 3.** (Color online): (a) Radial distribution function (RDF),  $g_i(r)$ , and (b) mean electrostatic potential,  $\Psi(r)$ , as a function of the distance to the surface of an infinite uncharged cylinder immersed in a  $-1:+3$  electrolyte. Symbols and lines correspond to MC simulations and the MPB theory, respectively. The blue circles and the blue solid line correspond to the RDF of monovalent anions; the black squares and the black dashed line correspond to the RDF of trivalent cations; the green triangles and the green dot-dashed line are associated to the mean electrostatic potential. The monovalent anions have a concentration  $\rho^{bulk} = 1M$ , and the concentration of cations is adjusted, accordingly, in order to fulfill the electroneutrality condition as a function of their valence  $z_+$ .

the monotonic decreasing of  $\tau_c$  indicates a shrinking of the electrical double layer as a function of  $\sigma_0$ . This behaviour is also consistent with the monotonic curvature of  $\Psi_H$  observed in Fig. 1(a) according to Eq. (46) by noting that  $\frac{d^2\Psi_0}{d\sigma_0^2}$  does not change its sign. On the other hand, the  $\tau_c$  for the linearized Poisson-Boltzmann (or Debye-Hückel) theory displays a constant value, which is also attained by the NLPB equation at  $\sigma_0 = 0$  as expected. This convergence of the numerical NLPB results to the analytical Debye-Hückel values is observed in all  $1 : z$  electrolytes, as it can be seen in Figs. 4(b) and 4(c). The MPB results agree well with the MC results specially at high values of  $\sigma_0$ , whereas the HNC/MSA integral equations results coincide very well with the MC results at low and intermediate values of  $\sigma_0$ .

In Fig. 4(b) for a  $-1 : +2$  system, the  $\tau_c$  displays a non-monotonic behaviour as a function of  $\sigma_0$  according to MC simulations and all the theories. Near  $\sigma_0 = 0$ ,  $\tau_c$  increases as a function of  $\sigma_0$  until a maximum is reached at a critical surface charge density given by the equation

$$\frac{\Psi_0}{\sigma_0} = \left( \frac{d\Psi_0}{d\sigma_0} \right). \tag{55}$$

**Table 1**

Mean electrostatic potential at the surface of an uncharged cylinder,  $\Psi_0(\sigma_0 = 0)$ , immersed in a  $-1 : z_+$  electrolyte. The monovalent anions have the same concentration  $\rho_{-}^{bulk} = 1$  M in all instances, and the concentration of cations is adjusted, accordingly, in order to fulfill the electroneutrality condition as a function of its valence  $z_+$ .

$z_-$	$z_+$	NLPB [mV]	HNC/MSA [mV]	MPB [mV]	MC [mV]
-1	+2	0	0	-1.76	-1.7
-1	+3	0	0	-4.50	-4.0

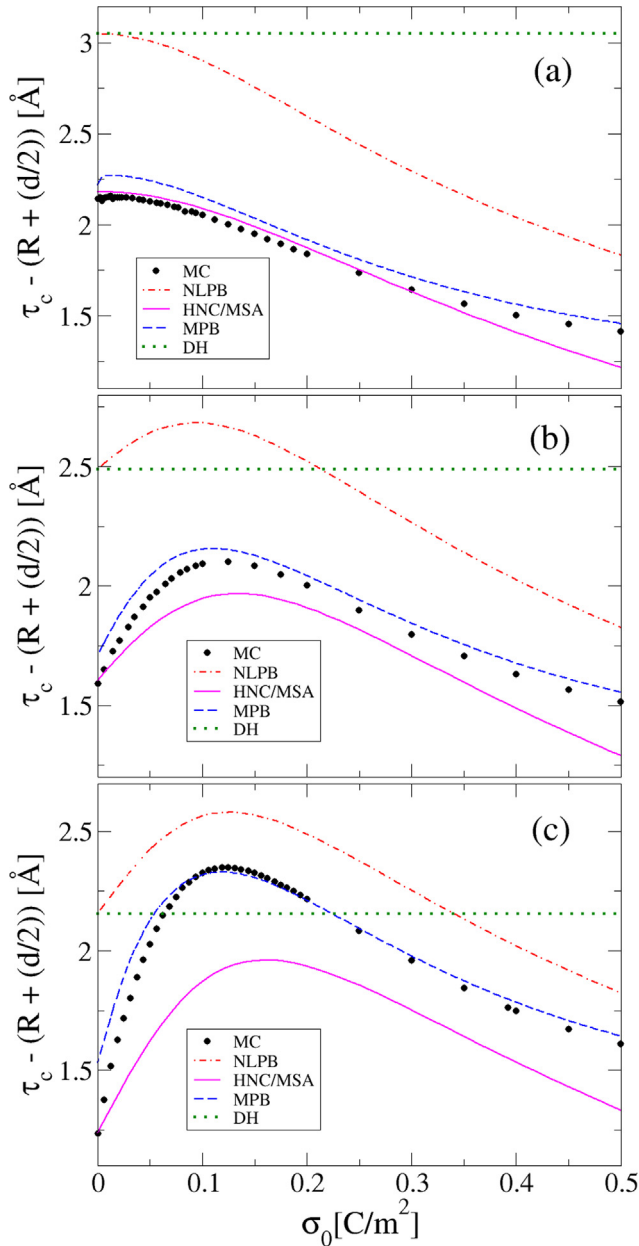


**Fig. 4.** (Color online): Capacitive compactness,  $\tau_c$ , as a function of the surface charge density,  $\sigma_0$ , in the presence of the following  $-1 : z_+$  electrolytes: (a)  $-1 : +1$ , (b)  $-1 : +2$ , and (c)  $-1 : +3$ . Solid circles, dot-dashed lines, solid lines, dashed lines, and dotted lines correspond to MC simulations, NLPB equation, integral equations in the HNC/MSA approximation, the MPB theory, and the analytic Debye-Hückel approximation (see Eq. (52)), respectively. The monovalent anions have the same concentration  $\rho_{-}^{bulk} = 1$  M in all instances, and the concentration of cations is adjusted, accordingly, in order to fulfill the electroneutrality condition as a function of their valence  $z_+$ .

In addition, at the critical surface charge density  $\sigma_0'$

$$\frac{d\tau_c}{d\sigma_0} = \frac{d^2\Psi_0}{d\sigma_0^2} = \frac{d^2\tau_c}{d\sigma_0^2} = 0. \quad (56)$$

For  $\sigma_0 > \sigma_0'$  it is seen that  $\tau_c$  decreases monotonically as a function of  $\sigma_0$ . As discussed previously [4], the increasing of  $\tau_c$  near  $\sigma_0 = 0$  is associated with an expansion of the electrical double layer, whereas the monotonic decreasing of  $\tau_c$  for  $\sigma_0 > \sigma_0'$  indicates a shrinking of the electrical double layer. The maximum of  $\tau_c$  corresponds to the point at which a change of curvature of  $\Psi_H$  occurs in Fig. 1 according to Eq. (56) by recalling that  $\Psi_0(\sigma_0) = \frac{\lambda}{2\pi\epsilon_0\epsilon} \ln\left(1 + \frac{d/2}{R}\right) + \Psi_H(\sigma_0)$ . Interestingly, the NLPB results predict qualitatively the same behaviour displayed by MC simulations. The MPB results reproduce the MC results well specially at intermediate and high values of  $\sigma_0$ , whereas the HNC/MSA integral equations data agree well with the simulations specially near  $\sigma_0 = 0$ .

For a 1:3 system in Fig. 4(c),  $\tau_c$  shows a similar non-monotonic behaviour to that observed in Fig. 4(b) as a function of  $\sigma_0$ . Near  $\sigma_0 = 0$  we have  $\tau_c$  increasing until a maximum is reached at a critical  $\sigma_0'$ , whereas for  $\sigma_0 > \sigma_0'$  it is seen that  $\tau_c$  decreases monotonically. The maximum of  $\tau_c$  at  $\sigma_0'$  corresponds to the point at which a change of curvature of  $\Psi_H$  occurs in Fig. 1(c). Here, however, the increase of the anion's valence from  $z_+ = +2$  to  $z_+ = +3$  decreases the value of  $\tau_c$  at  $\sigma_0 = 0$ , and increases the difference between the maximum value of  $\tau_c$  and the value of  $\tau_c$  at  $\sigma_0 = 0$ . In all the three cases in Fig. 4, the MPB values for  $\tau_c$  in the neighbourhood of  $\sigma_0 = 0$  are slightly larger than the MC results. This is due to the approximations in calculating the fluctuation potential and the choice of the planar exclusion volume term, see Eq. (13).

In order to analyze the non-dominance of counterions, in Fig. 5 we have plotted the difference of the surface mean electrostatic potential  $\Delta_{-1:z_+}^{-1:+1}\Psi_0 = \Psi_0^{-1:+1} - \Psi_0^{-1:z_+}$ , where  $\Psi_0^{-1:+1}$  and  $\Psi_0^{-1:z_+}$  correspond to the mean electrostatic potential on the electrode's surface  $\Psi_0$  in the presence of a  $-1 : +1$  and a  $-1 : z_+$  electrolyte, respectively, when the properties of counterions in both electrolytes are the same. In this figure, it is observed that  $\Delta_{-1:z_+}^{-1:+1}\Psi_0$  tends to the same finite value at  $\sigma_0 = 0$  according to MC simulations and the MPB theory, whereas the NLPB equation and the HNC/MSA integral equations predict a zero value for  $\Delta_{-1:z_+}^{-1:+1}\Psi_0$  if the colloidal surface is uncharged. The NLPB  $\Delta_{-1:z_+}^{-1:+1}\Psi_0$  remains positive and tends to zero in the limit of an infinite surface charge density  $\sigma_0$ . An analogous behaviour has been observed in planar geometry [7]. Contrastingly, MC simulations, the HNC/MSA and the MPB results show that the  $\Delta_{-1:z_+}^{-1:+1}\Psi_0$  does not converge to zero at large  $\sigma_0$  values. Moreover, the MC data show a change of sign of  $\Delta_{-1:z_+}^{-1:+1}\Psi_0$  around the particular surface charge density  $\sigma_0' \approx 0.15$  C/m<sup>2</sup> for  $\Delta_{-1:z_+}^{-1:+1}\Psi_0$  and around  $\sigma_0' \approx 0.125$  C/m<sup>2</sup> for  $\Delta_{-1:z_+}^{-1:+1}\Psi_0$ , according Monte Carlo simulations. Notice that also the MPB and HNC/MSA theories display a similar change of sign. This means that there is change of precedence in the surface mean electrostatic potential as a function of  $\sigma_0$ :  $\Psi_0^{-1:+1} > \Psi_0^{-1:z_+}$  if  $\sigma_0 < \sigma_0'$  whereas  $\Psi_0^{-1:+1} < \Psi_0^{-1:z_+}$  if  $\sigma_0 > \sigma_0'$ . A similar change of precedence of the surface mean electrostatic potential as a function of  $\sigma_0$  at the Helmholtz plane has been reported in Ref. [15] in planar and spherical geometry.

The difference of the capacitive compactness  $\Delta_{-1:z_+}^{-1:+1}\tau_c = \tau_0^{-1:+1} - \tau_0^{-1:z_+}$  is plotted in Fig. 6. As can be observed, the  $\Delta_{-1:z_+}^{-1:+1}\tau_c$  tends approximately to the same finite value at

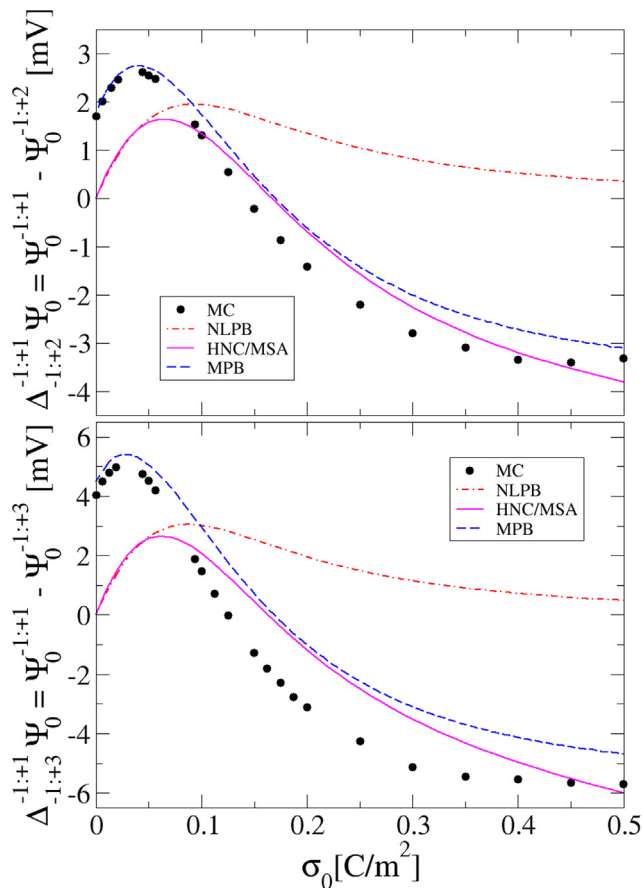


**Fig. 5.** (Color online): Difference of the surface mean electrostatic potential,  $\Delta_{-1:z_+}^{-1:z_+} \Psi_0 = \Psi_0^{-1:z_+} - \Psi_0^{-1:z_+}$ , where  $\Psi_0^{-1:z_+}$  and  $\Psi_0^{-1:z_+}$  correspond to the mean electrostatic potential on the electrode's surface in the presence of a  $-1 : +1$  and a  $-1 : z_+$  electrolyte, respectively. The monovalent anions have the same concentration  $\rho_{-}^{bulk} = 1M$  in all instances, and the concentration of cations is adjusted, accordingly, in order to fulfill the electroneutrality condition as a function of their valence  $z_+$ .

$\sigma_0 = 0$  according to MC simulations and the theories for  $z_+ = +2$ . For  $z_+ = +3$  the MPB theory underestimates the corresponding MC values at  $\sigma_0 = 0$ . This is again due to the use of an approximate fluctuation potential and the planar exclusion volume as noted in the overestimate of  $\tau_c$  in Fig. 4 at small  $\sigma_0$ . The NLPB  $\Delta_{-1:z_+}^{-1:z_+} \tau_c$  is always positive decreasing monotonically to zero in the limit of an infinite surface charge density  $\sigma_0$ . An analogous behavior has been reported in planar geometry [7] according to the NLPB theory. In contrast, MC simulations, the HNC/MSA and the MPB results show a change of sign of  $\Delta_{-1:z_+}^{-1:z_+} \tau_c$ . In particular, the MC data show a change of sign of  $\Delta_{-1:z_+}^{-1:z_+} \tau_c$  around the particular surface charge density  $\sigma_0'' \approx 0.09C/m^2$  for  $\Delta_{-1:z_+}^{-1:z_+} \Psi_0$  and around  $\sigma_0'' \approx 0.075C/m^2$  for  $\Delta_{-1:z_+}^{-1:z_+} \Psi_0$ . This indicates that there is change of precedence of the capacitive compactness as a function of  $\sigma_0$ :  $\tau_c^{-1:z_+} > \tau_c^{-1:z_+}$  if  $\sigma_0 < \sigma_0''$  whereas  $\tau_c^{-1:z_+} < \tau_c^{-1:z_+}$  if  $\sigma_0 > \sigma_0''$ , with  $\sigma_0''$  being the crossover surface charge density.

#### 4. Conclusions

In this work, we have proposed a generalization of the capacitive compactness of the electrical double layer when there is a

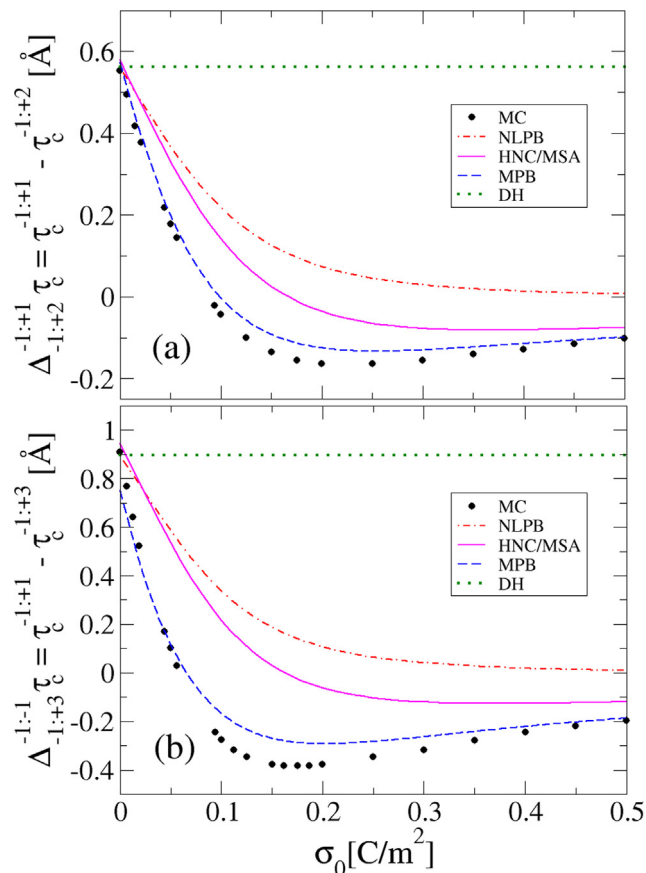


**Fig. 6.** (Color online): Difference of the capacitive compactness,  $\Delta_{-1:z_+}^{-1:z_+} \tau_c = \tau_c^{-1:z_+} - \tau_c^{-1:z_+}$ , where  $\tau_c^{-1:z_+}$  and  $\tau_c^{-1:z_+}$  correspond to the capacitive compactness in the presence of a  $-1 : +1$  and a  $-1 : z_+$  electrolyte, respectively. The monovalent anions have the same concentration  $\rho_{-}^{bulk} = 1M$  in all instances, and the concentration of cations is adjusted accordingly in order to fulfill the electroneutrality condition as a function of its valence  $z_+$ .

non-zero surface mean electrostatic potential (or pzc) around an uncharged colloid. These non-zero pzc's for divalent and trivalent coions have been predicted by the MPB theory and supported by the MC simulations. Increasing the coion charge from 2 to 3 increases the pzc. Non-zero pzc's for 1:2 salts have been observed in the MPB theory for planar and spherical double layers [39,40]. The predictions of the MPB theory for the mean electrostatic potential, in general, are also closer to the simulations than that due to the other theories. Admittedly, the MPB singlet distribution functions display a discontinuity in the gradient at a distance  $3d/2$  from the surface of the cylinder, which arises from the approximate calculation of the fluctuation potential. This discontinuity is clearly an artifact of the theory. Neither the HNC/MSA nor NLPB theory predicts a pzc. The failure of the HNC/MSA integral equation is probably due to the neglect of the interplay between the ion correlations and excluded volume effects in the MSA bulk direct correlation function  $c_{ij}(r)$ , when the ions are in the neighbourhood of the cylinder.

The pzc results from the breaking of the valence symmetry of size-symmetric electrolytes with multivalent coions. In such a scenario, the capacitive compactness displays a maximum as a function of the surface charge density, suggesting an expansion and shrinking of the electrical double layer in the presence of ion correlations and ionic excluded volume effects, and also, notably, in the NLPB theory. A change of precedence of the surface (and

Helmholtz) mean electrostatic potential and the capacitive compactness for  $-1 : z_+$  electrolytes regarding  $-1 : +1$  salts has been clearly shown by MC simulations and the non-mean field MPB and HNC/MSA approaches. The NLPB theory is unable to predict these phenomena, illustrating the limitations of this mean field theory. On the other hand, both the HNC/MSA and MPB theories give the correct qualitative and semi-quantitative behaviour for the capacitive compactness, with the MPB being closer overall to the simulation results.

### Declaration of Competing Interest

The authors declare that they have no known competing financial interests or personal relationships that could have appeared to influence the work reported in this paper.

### Acknowledgements

G. I. G.-G. acknowledges the SEP-CONACYT CB-2016 grant 286105, the 2019 Marcos Moshinsky Fellowship, the National Supercomputing Center-IPICYT for the computational resources provided via the grant TKII-IVGU001, and the computing time granted by LANCAD and CONACYT in the Supercomputer Hybrid Cluster "Xihuhcoatl" at GENERAL COORDINATION OF INFORMATION AND COMMUNICATIONS TECHNOLOGIES (CGSTIC) of CINVESTAV with the project 13-2022. G.I. G.-G. and E. G.-T. acknowledge the SEP-CONACYT grant FOP16-2021-01-320091, and express their gratitude for the assistance from the computer technicians at the IF-UASLP.

### References

- [1] E. González-Tovar, F. Jiménez-Ángeles, René Messina, M. Lozada-Cassou, *J. Chem. Phys.* 120 (2004) 9782.
- [2] G.I. Guerrero-García, E. González-Tovar, M. Chávez-Páez, J. Klos, S. Lamperski, *Phys. Chem. Chem. Phys.* 20 (2018) 262–275.
- [3] C.L. Moraila-Martínez, G.I. Guerrero-García, M. Chávez-Páez, E. González-Tovar, *J. Chem. Phys.* 148 (2018) 154703.
- [4] G.I. Guerrero-García, E. González-Tovar, M. Chávez-Páez, Tao Wei, *J. Mol. Liq.* 277 (2019) 104–114.
- [5] C.N. Patra, *RSC Advances* 10 (2020) 39017–39025.
- [6] E. González-Tovar, J.A. Martínez-González, C.G. Galván Peña, G.I. Guerrero-García, *J. Chem. Phys.* 154 (2021) 096101.
- [7] J.J. Elisea-Espinoza, E. González-Tovar, J.A. Martínez-González, C.G. Galván Peña, G.I. Guerrero-García, *Mol. Phys.* 119 (2021) e1916633.
- [8] R.J. Hunter, *Zeta Potential in Colloid Science*, Academic Press, New York, 1981.
- [9] R.J. Hunter, *Foundations of Colloid Science*, Clarendon, Oxford, 1987.
- [10] W.B. Russell, D.A. Saville, W.R. Schowalter, *Colloidal Dispersions*, Cambridge University Press, Cambridge, UK, 1989.
- [11] G.I. Guerrero-García, E. González-Tovar, M. Lozada-Cassou, F.J. Guevara-Rodríguez, *J. Chem. Phys.* 123 (2005) 034703.
- [12] G.I. Guerrero-García, E. González-Tovar, M. Chávez-Páez, *Phys. Rev. E* 80 (2009) 021501.
- [13] G.I. Guerrero-García, E. González-Tovar, M. Olvera de la Cruz, *Soft Matter* 6 (2010) 2056–2065.
- [14] J.P. Valleau, G.M. Torrie, *J. Chem. Phys.* 76 (1982) 4623.
- [15] G.I. Guerrero-García, E. González-Tovar, M. Quesada-Pérez, A. Martín-Molina, *Phys. Chem. Chem. Phys.* 18 (2016) 21852–21864.
- [16] C.W. Outhwaite, *J. Chem. Soc. Faraday Trans. II* 82 (1986) 789.
- [17] L.B. Bhuiyan, C.W. Outhwaite, in: L. Blum, F.B. Malik (Eds.), *Condens. Matter Theor.*, Vol. 8, Plenum, New York, 1993, p. 551.
- [18] L.B. Bhuiyan, C.W. Outhwaite, *Philos. Mag. B* 69 (1994) 1051.
- [19] V. Dorvilien, C.N. Patra, L.B. Bhuiyan, C.W. Outhwaite, *Condens. Matter Phys.* 16 (43801) (2013) 1–12.
- [20] E. González-Tovar, M. Lozada-Cassou, L. Bari Bhuiyan, C.W. Outhwaite, *J. Mol. Liq.* 270 (2018) 157–167.
- [21] E. Gonzales-Tovar, M. Lozada-Cassou, D. Henderson, *J. Chem. Phys.* 83 (1985) 361.
- [22] Z. Ovanesyanyan, B. Medasani, M.O. Fenley, G.I. Guerrero-García, M. Olvera de la Cruz, M. Marucho, *J. Chem. Phys.* 141 (2014) 225103.
- [23] C.W. Outhwaite, L.B. Bhuiyan, *J. Chem. Soc. Faraday Trans. II* 78 (1982) 775.
- [24] R.E. Bellman, R.E. Kalaba, *Quasilinearization and Nonlinear Boundary-Value Problems*, American Elsevier Publishing Company, New York, 1965.
- [25] C.W. Outhwaite, in: K. Singer (Ed.), *A Specialist Periodical Reports – Statistical Mechanics*, Vol. 2, The Chemical Society, London, 1975, pp. 188–255.
- [26] K. Hiroike, *Mol. Phys.* 33 (1977) 1195–1198.
- [27] L. Mier-y-Terán, E. Díaz-Herrera, M. Lozada-Cassou, R. Saavedra-Barrera, *J. Comput. Phys.* 84 (1989) 326–342.
- [28] E. González-Tovar, M. Lozada-Cassou, *J. Phys. Chem.* 93 (1989) 3761–3768.
- [29] M.P. Allen, D.J. Tildesley, *Computer Simulation of Liquids*, Oxford University Press, New York, USA, 1989.
- [30] D. Frenkel, B. Smit, *Understanding Molecular Simulation*, Academic, London, 2002.
- [31] I. Fukuda, Y. Yonezawa, H. Nakamura, *J. Chem. Phys.* 134 (2011) 164107.
- [32] G. Vernizzi, G.I. Guerrero-García, M.O. de la Cruz, *Phys. Rev. E* 84 (2011) 016707.
- [33] I. Fukuda, H. Nakamura, *Biophys. Rev.* 4 (2012) 161.
- [34] P.X. Viveros-Mendez, A. Gil-Villegas, *J. Chem. Phys.* 136 (2012) 154507.
- [35] N. Kamiya, I. Fukuda, H. Nakamura, *Chem. Phys. Lett.* 568 (2013) 26.
- [36] J.M. Falcón-González, C. Contreras-Aburto, M. Lara-Peña, M. Heinen, C. Avendaño, A. Gil-Villegas, R. Castañeda-Priego, *J. Chem. Phys.* 153 (2020) 234901.
- [37] G.I. Guerrero-García, E. González-Tovar, M.O. de la Cruz, *J. Chem. Phys.* 135 (2011) 054701.
- [38] G.I. Guerrero-García, *Biophys. Chem.* 282 (2022) 106747.
- [39] C.W. Outhwaite, L.B. Bhuiyan, *Mol. Phys.* 74 (1991) 367.
- [40] L.B. Bhuiyan, C.W. Outhwaite, *Phys. Chem. Chem. Phys.* 6 (2004) 3467.